# Scattering Characteristics of Stratified Double Negative Stacks Using the Frequency Dispersive Cold Plasma Medium

Cumali Sabah and Savas Uckun

University of Gaziantep, Electrical and Electronics Engineering Department, 27310, Gaziantep, Turkey

Reprint requests to C. S.; E-mail: sabah@gantep.edu.tr

Z. Naturforsch. 62a, 247 - 253 (2007); received February 5, 2007

We present the wave propagation through stratified double negative stacks to illustrate the scattering characteristics of their structure. The double negative stacks are modeled by using the hypothetical non-dispersive and the frequency dispersive cold plasma media. The stacks are embedded between two double positive media and the incident electric field is assumed a plane electromagnetic wave with any arbitrary polarization. By imposing the boundary conditions, the relations between the fields inside and outside the stacks can be written in a matrix form. Using this transfer matrix, the incident, reflected, and transmitted powers are derived. The variations of the powers for the stratified double negative stacks using the frequency dispersive cold plasma medium have not been investigated yet, in detail. Thus, their characteristics for the perpendicular polarization is computed and presented in numerical results with the emphasis on the plasma frequencies. It is seen from the numerical results that the stratified double negative stacks can be used as electromagnetic filters at some frequency bands

Key words: Double Negative Medium; Cold Plasma; Frequency Dispersive; Reflection and Transmission; Propagation.

### 1. Introduction

Since a few years, so-called double negative (DNG) media became interesting because of their potential application in some microwave, millimeter-wave and optical frequency bands. These media, not commonly found in nature, have simultaneously negative permittivity and permeability in a limited frequency band. Negative permittivity could be realized by periodic rods and negative permeability by split-rings over a certain frequency band. The DNG medium was first suggested by Veselago in 1968 [1]. Such a medium is theoretically characterized in his study, and the propagation of the waves in hypothetical lossless DNG material is analyzed. Then, Pendry and his co-workers [2] demonstrated that a very simple metallic microstructure, comprising a regular array of thin wires, exhibits novel electromagnetic properties in the GHz region, analogous to those exhibited by a solid metal in the ultraviolet range. In 1999, Pendry and his group [3] showed that microstructures, built from non-magnetic conducting sheets, exhibit an effective magnetic permeability, which can be tuned to values not accessible in naturally occurring materials, including large imaginary components of effective magnetic permeability. In 2000, Smith and his co-workers [4] presented and constructed a composite medium, based on a periodic array of interspaced conducting nonmagnetic split-ring resonators and continuous wires, that exhibits a frequency region in the microwave regime with simultaneously negative values of effective permeability and permittivity. In 2001, Shelby et al. [5] performed the first experiment that showed the scattering data at microwave frequencies on such a structured so-called "metamaterial", that exhibits a frequency band where the effective index of refraction is negative. The results of this experiment, done for the negative refraction, were criticized by Valanju et al. in 2002 [6]. They stated that negative refraction is impossible for any real physical signal within a finite bandwidth. This statement was found incorrect by Pendry and Smith in 2003 [7]. Moreover, studies on DNG materials, such as multilayer DNG media, have been performed by many researchers [8-12]. The topic continues to be of great interest and practical importance due to a variety of potential applications (many studies can be found in [13]).

Following a brief overview of the history of DNG materials, we talk about how the DNG medium is char-

0932-0784 / 07 / 0500-0247 \$ 06.00 © 2007 Verlag der Zeitschrift für Naturforschung, Tübingen · http://znaturforsch.com

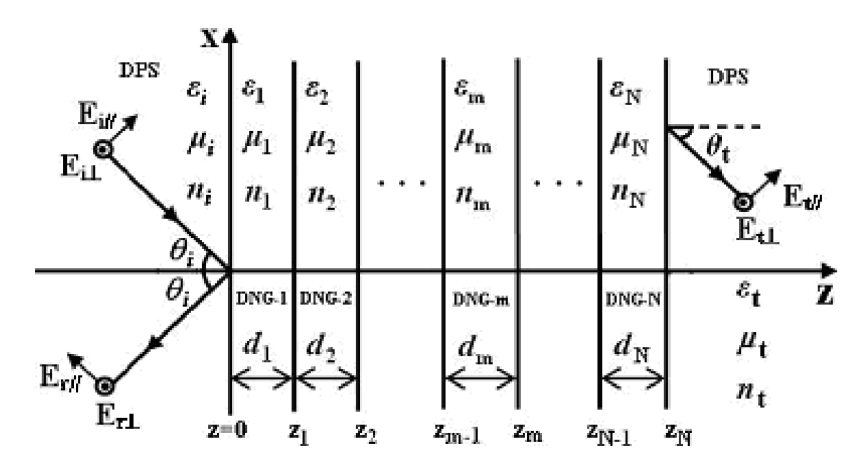


Fig. 1. Configuration of stratified DNG stacks.

acterized mathematically. In the literature, the DNG medium is usually described by using the Lorentz, Drude, Debye, and/or cold plasma parameters as in [1-5, 11, 14-21]. In this work, we use the cold plasma parameters as in [14] and [15] to characterize the DNG stacks.

In this study, we analyzed the scattering characteristics of stratified double negative stacks, using the frequency dispersive cold plasma medium extensively. We describe the stratified DNG stacks as a structure similar to the multilayer dielectric slabs and investigate their scattering behaviour in the theoretical analysis and the numerical results. Theoretically, the stratified DNG stacks are considered to form N pieces frequency dispersive DNG layers with different material properties and thicknesses. The incident electric field is assumed to be a plane electromagnetic wave with any arbitrary polarization. After examining the electric and magnetic fields, using Maxwell's equations both inside and outside the DNG stacks, and imposing the boundary conditions, we can determine the incident, reflected, and transmitted powers to observe their features. Although the wave interaction with multilayer DNG media is studied in the literature, the powers and their variations for the stratified double negative stacks made from the frequency dispersive cold plasma medium have not been investigated yet. Thus, the behaviour of the powers for the perpendicular polarization against the incidence angle and the frequency is computed and presented in numerical results with emphasis on the plasma frequencies. From the numerical results one can see that the stratified structure can be used as electromagnetic filters in some frequency regions.

# 2. Theoretical Analysis

A DNG medium has interesting properties when it is composed of stratified DNG stacks embedded between two double positive (DPS) media. We consider any arbitrary polarization plane of an electromagnetic incident electric field from free-space that is encountering the dielectric DNG stack interface. The stratified DNG stack considered in this paper is composed of N frequency dispersive DNG layers with different material properties and thicknesses, as shown in Figure 1. In the analysis,  $\exp(j\omega t)$  time dependence is assumed and suppressed throughout this work.

Referring to Fig. 1, the incident electric field with any arbitrary polarization can be written as

$$\mathbf{E}_{i} = [E_{i\parallel}(\cos\theta_{i}\mathbf{a}_{x} + \sin\theta_{i}\mathbf{a}_{z}) + E_{i\perp}\mathbf{a}_{y}] \\ \cdot \exp[-j(-k_{iy}x + k_{iz}z)],$$
(1)

where  $\theta_i$  is the angle of the incidence,  $k_{ix}$  (=  $k_i \sin \theta_i$ ) and  $k_{iz}$  (=  $k_i \cos \theta_i$ ) are the x- and z-components of the wave number  $k_i$  (=  $\omega \sqrt{\mu_i \varepsilon_i}$ ). Note that, the subscripts  $\parallel$  and  $\perp$  refer to the parallel and perpendicular components of the electric field vector, respectively. According to the incident electric field given in (1), the reflected ( $\mathbf{E}_r$ ) and the transmitted ( $\mathbf{E}_t$ ) electric fields can be expressed as

$$\boldsymbol{E}_{r} = [E_{r\parallel}(\cos\theta_{i}\boldsymbol{a}_{x} - \sin\theta_{i}\boldsymbol{a}_{z}) + E_{r\perp}\boldsymbol{a}_{y}] \\ \cdot \exp[-j(-k_{ix}x - k_{iz}z)],$$
(2)

$$\boldsymbol{E}_{t} = [E_{t\parallel}(\cos\theta_{t}\boldsymbol{a}_{x} + \sin\theta_{t}\boldsymbol{a}_{z}) + E_{t\perp}\boldsymbol{a}_{y}] \\ \cdot \exp[-j(-k_{tx}x + k_{tz}z)],$$
(3)

where  $\theta_t$  is the transmission angle,  $k_t = \omega \sqrt{\mu_i \varepsilon_t}$  is the wave number of the transmitted medium,

 $k_{tx}$  (=  $k_t \sin \theta_t$ ) and  $k_{tz}$  (=  $k_t \cos \theta_t$ ) are the x- and z-components of the wave number  $k_t$ .

The electric field in any stack reflects and transmits to another stack upon reaching the transmitted medium. Therefore, in the  $m^{\rm th}$  DNG stack there are two waves, one propagating toward the right interface and the other one propagating toward the left interface. Thus, in the  $m^{\rm th}$  DNG stack, the total electric field can be stated as

$$\begin{aligned} \boldsymbol{E}_{m} &= \left[ A_{\parallel} (\cos \theta_{m} \boldsymbol{a}_{x} + \sin \theta_{m} \boldsymbol{a}_{z}) + A_{\perp} \boldsymbol{a}_{y} \right] \\ &\cdot \exp[-j(-k_{mx}x + k_{mz}z)] \\ &+ \left[ B_{\parallel} (\cos \theta_{m} \boldsymbol{a}_{x} - \sin \theta_{m} \boldsymbol{a}_{z}) + B_{\perp} \boldsymbol{a}_{y} \right] \\ &\cdot \exp[-j(-k_{mx}x - k_{mz}z)], \end{aligned} \tag{4}$$

where  $A_{\parallel}$ ,  $A_{\perp}$ ,  $B_{\parallel}$ , and  $B_{\perp}$  are the amplitudes of the electric fields inside the  $m^{\text{th}}$  DNG stack,  $\theta_m$  is the refracted angle,  $k_m$  is the wave number of the  $m^{\text{th}}$  DNG stack,  $k_{mx}$  (=  $k_m \sin \theta_m$ ) and  $k_{mz}$  (=  $k_m \cos \theta_m$ ) are the x- and z-components of the wave number  $k_m$ . Note that in all representations, the subscripts i, m, and t stand for the incident medium, the  $m^{\text{th}}$  DNG stack, and the transmitted medium, respectively. In addition, the wave number of the  $m^{\text{th}}$  DNG stack must be negative and can be given as

$$k_m = -\omega\sqrt{\mu_m \varepsilon_m}. (5)$$

Here, the permeability  $\mu_m$  and the permittivity  $\varepsilon_m$  for the  $m^{\text{th}}$  DNG stack are defined using the frequency dispersive cold plasma parameters to obtain the simultaneously negative permittivity and permeability in a certain frequency band [13, 14]. So, they can be given as

$$\mu(\omega) = \mu_{\rm o} \left( 1 - \frac{f_{\rm mp}^2}{f^2} \right),\tag{6}$$

$$\varepsilon(\omega) = \varepsilon_{\rm o} \left( 1 - \frac{f_{\rm ep}^2}{f^2} \right),$$
 (7)

where  $f_{\rm mp}$  is the magnetic plasma frequency and  $f_{\rm ep}$  the electronic plasma frequency. The parameters given in (6) and (7) have frequency-dependent characteristics which provide to obtain simultaneously negative permeability and permittivity in a certain frequency range. If these equations are used in (5), it is seen that the wave number  $k_m$  has also a frequency-dependent characteristic as the permeability and permittivity of the cold plasma medium. These allow to use the frequency dispersive cold plasma as a DNG stack. Furthermore,

to obtain the simultaneously negative values for the permeability and permittivity, the conditions  $f_{\rm mp} > f$  and  $f_{\rm ep} > f$  must be satisfied.

To solve the general problem for the incident, reflected, and transmitted power for the stratified DNG stacks shown in Fig. 1 it is necessary to investigate the interfaces between DPS-DNG media and two DNG media. Thus, imposing the boundary conditions at the interfaces z = 0,  $z = z_m$  (m = 1, 2, 3, ..., N - 1) and  $z = z_N$ , the relationships among the fields in all regions can be obtained by the transfer matrix [U] as in [11] and [12], which is expressed as

$$\begin{bmatrix} E_{i\perp} \\ E_{r\perp} \\ E_{i\parallel} \\ E_{r\parallel} \end{bmatrix} = [U] \begin{bmatrix} E_{t\perp} \\ E_{t\parallel} \end{bmatrix} = \begin{bmatrix} u_{11} & u_{12} \\ u_{21} & u_{22} \\ u_{31} & u_{32} \\ u_{41} & u_{42} \end{bmatrix} \begin{bmatrix} E_{t\perp} \\ E_{t\parallel} \end{bmatrix}, \quad (8)$$

where  $[U] = [A] [B_1] [B_2] [B_3] \cdots [B_m] \cdots [B_{N-1}] [C]$ . Note that, [A] and  $[B_m]$  are both square matrices of order 4, [C] is a  $4 \times 2$  matrix and [U] is in the form of a  $4 \times 2$  matrix. The elements of [A],  $[B_m]$ , and [C] are expressed as a function of the incidence angle, the structure parameters, the thickness of each DNG stack, and the frequency. Then, according to (8), we can write the reflected and the transmitted electric fields in terms of the incident electric field as

$$E_{\rm r\perp} = \frac{(u_{21}u_{32} - u_{22}u_{31})E_{\rm i\perp} + (u_{11}u_{22} - u_{12}u_{21})E_{\rm i\parallel}}{(u_{11}u_{32} - u_{12}u_{21})},$$
(9)

$$E_{\rm r\parallel} = \frac{(u_{32}u_{41} - u_{31}u_{42})E_{\rm i\perp} + (u_{11}u_{42} - u_{12}u_{41})E_{\rm i\parallel}}{(u_{11}u_{32} - u_{12}u_{21})},$$
(10)

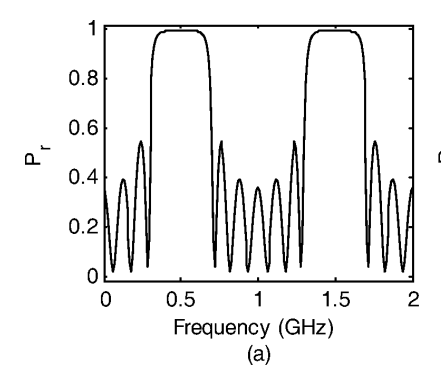
$$E_{\mathsf{t}\perp} = \frac{(u_{32})E_{\mathsf{i}\perp} - (u_{12})E_{\mathsf{i}\parallel}}{(u_{11}u_{32} - u_{12}u_{21})},\tag{11}$$

$$E_{t\parallel} = \frac{-[(u_{31})E_{i\perp} - (u_{11})E_{i\parallel}]}{(u_{11}u_{32} - u_{12}u_{21})},$$
(12)

where  $u_{ab}$  (a = 1, 2, 3, 4; b = 1, 2) are the elements of the  $4 \times 2$  transfer matrix [U].

Now, the *z*-component of the incident, reflected, and transmitted powers can be represented as

$$|m{P}_{\mathrm{i}z}| = \left|rac{k_{\mathrm{i}z}}{2\mu_{\mathrm{i}}}(E_{\mathrm{i}\perp}^2 + E_{\mathrm{i}\parallel}^2)
ight|,$$



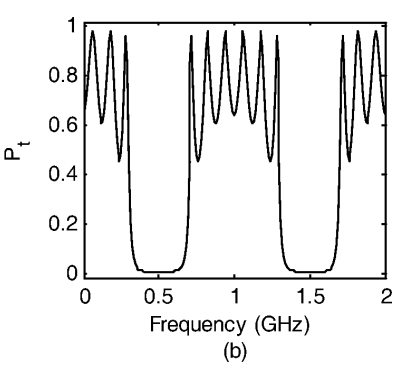


Fig. 2. Reflected and transmitted powers of the seven non-dispersive DNG stacks as a function of the frequency at normal incidence.

$$\begin{aligned} |\boldsymbol{P}_{\mathrm{rz}}| &= \left| \frac{k_{\mathrm{i}z}}{2\mu_{\mathrm{i}}} (E_{\mathrm{r}\perp}^2 + E_{\mathrm{r}\parallel}^2) \right|, \quad \text{and} \\ |\boldsymbol{P}_{\mathrm{tz}}| &= \left| \frac{k_{\mathrm{tz}}}{2\mu_{\mathrm{t}}} (E_{\mathrm{t}\perp}^2 + E_{\mathrm{t}\parallel}^2) \right|. \end{aligned} \tag{13}$$

If the incident electric field is normalized to unity, the conservation of the power yields

$$|(E_{\rm r\perp}^2 + E_{\rm r\parallel}^2)| + \left| \frac{k_{\rm tz}\mu_{\rm i}}{k_{\rm iz}\mu_{\rm t}} \right| \cdot |(E_{\rm t\perp}^2 + E_{\rm t\parallel}^2)| = 1.$$
 (14)

#### 3. Numerical Results

In this section we carry out the computations for the powers to observe the characteristics of them, using the results obtained in Section 2, when the incident power is normalized to unity. To verify the computations, the conservation of power, as a first method, given in (14) is satisfied for all examples. As a second method, an equivalent transmission line is obtained for the structure given in Fig. 1 [22]. Both methods give the same numerical values for all computations. Thus, the results are verified by means of two methods.

# 3.1. Example I

Here, we intend to find the characteristics of nondispersive DNG stacks. It is also worth mentioning that, although the cold plasma medium has the frequency-dependent parameters given in (6) and (7), both parameters are assumed to be constant over a frequency band in this example. To do this,  $f_{\rm mp}$  and  $f_{\rm ep}$ must be expressed as a function of the frequency f like  $f_{\rm mp}=c_1f$  and  $f_{\rm ep}=c_2f$ . Note that  $c_1$  and  $c_2$  must be real constants and greater than one to get a negative permittivity and permeability for the DNG stacks. This is the hypothetical approximation which allows making a comment on the effect of the frequency for the non-dispersive DNG stack characteristics. Note that the non-dispersive and negative permittivity and permeability were used in many studies, as in [8–14].

The reflected  $(P_r)$  and transmitted  $(P_t)$  powers for the seven non-dispersive DNG stacks are calculated as a function of the frequency and the incidence angle, when the incident electric field is a plane electromagnetic wave with perpendicular polarization ( $E_{\parallel}=0$ ). The incident and transmitted media are assumed to become free-space, and Germanium with  $\mu_i = \mu_t = \mu_o$ ,  $\varepsilon_i = \varepsilon_o$  and  $\varepsilon_t = 16\varepsilon_o$ . The operation frequency is selected to be  $f_0 = 1.0$  GHz. The seven non-dispersive DNG stacks are composed of two media H and L as  $(HL)^3H$ , where  $\mu_H = \mu_L = -\mu_o$ ,  $\varepsilon_H = -9\varepsilon_o$  and  $\varepsilon_{\rm L} = -\varepsilon_{\rm o}$ , in which  $f_{\rm mp} = \sqrt{2}f$  and  $f_{\rm ep} = \sqrt{10}f$  for the H medium, and  $f_{\rm mp} = f_{\rm ep} = \sqrt{2}f$  for the L medium. The thicknesses  $d_{\rm H}$  and  $d_{\rm L}$  are arranged from  $|n_{\rm H}d_{\rm H}|=$  $|n_{\rm L}d_{\rm L}| = \lambda_{\rm o}/2$ , where  $n_{\rm H}$  and  $n_{\rm L}$  are the refractive indices, and  $\lambda_0$  is the wavelength in free-space at the operation frequency.

Figure 2 points out the reflected and transmitted powers as a function of the frequency at normal incidence.  $P_{\rm r}$  shows a band-pass filter characteristic between the frequency regions 0.28-0.72 GHz and 1.28-1.72 GHz. On the other hand,  $P_{\rm t}$  reaches to unity between the ranges of 0-0.28 GHz, 0.72-1.28 GHz, and 1.72-2 GHz, and shows a saw-comb filter characteristic. It is said that, the frequency response of the non-dispersive DNG stacks acts as the band-pass and anti-reflection filters at some frequency regions for the given configuration.

Figure 3 displays the reflected and transmitted powers versus the incidence angle at the operation frequency. The reflected power is nearly constant between  $0^{\circ}$  and  $30^{\circ}$ , and then it increases up to unity. The transmitted power is dominant between  $0^{\circ}$  and  $50^{\circ}$ ; after that it decreases and becomes nearly zero after  $70^{\circ}$ .

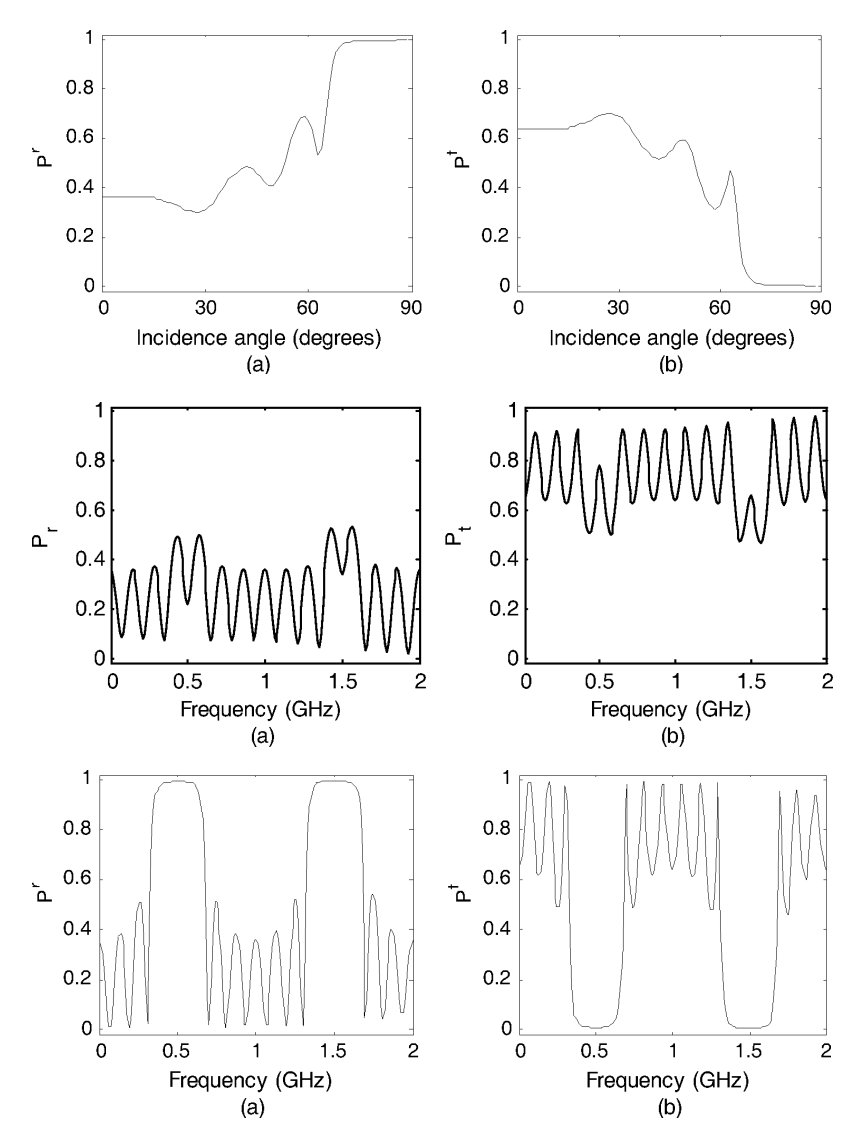


Fig. 3. Reflected and transmitted powers of the seven non-dispersive DNG stacks versus the incidence angle at the operation frequency.

Fig. 4. Reflected and transmitted powers of the seven frequency dispersive DNG stacks against the frequency at normal incidence with  $f_{\rm epH} = 5$  GHz,  $f_{\rm epL} = 4$  GHz, and  $f_{\rm mpH} = f_{\rm mpL} = 3$  GHz.

Fig. 5. Reflected and transmitted powers of the seven frequency dispersive DNG stacks against the frequency at normal incidence with  $f_{\rm epH}=10$  GHz,  $f_{\rm epL}=4$  GHz, and  $f_{\rm mpH}=f_{\rm mpL}=3$  GHz.

We can say that, after  $70^{\circ}$  there is no transmission, there is only reflection for the given example.

# 3.2. Example II

In this example, we desire to find out the characteristics of the frequency dispersive double negative stacks. The seven frequency dispersive DNG stacks are again considered as in the previous example to compute the reflected and transmitted powers as a function of the frequency and the incidence angle for the perpendicular polarization. The structure parameters for the incident, the DNG stacks, and the transmitted media are the same as the former one except for the permeability and permittivity of the DNG stacks. Here, they are cal-

culated using (6) and (7) with the appropriate plasma frequencies. In addition, the effect of the plasma frequencies is emphasized in this computation. In our calculation there are four plasma frequencies, two for the H medium and the other two for the L medium. For emphasizing the effect of the plasma frequencies, three frequencies are fixed and the fourth one is varied.

Figure 4 corresponds to  $P_{\rm r}$  and  $P_{\rm t}$  against the frequency at normal incidence with  $f_{\rm epH} = 5$  GHz,  $f_{\rm epL} = 4$  GHz, and  $f_{\rm mpH} = f_{\rm mpL} = 3$  GHz. It is seen in this figure that  $P_{\rm r}$  and  $P_{\rm t}$  show an oscillatory behaviour at some frequency band. Furthermore, the given structure transmits most of the incident wave, because  $P_{\rm t}$  is greater than  $P_{\rm r}$  in a wide range of the frequency.

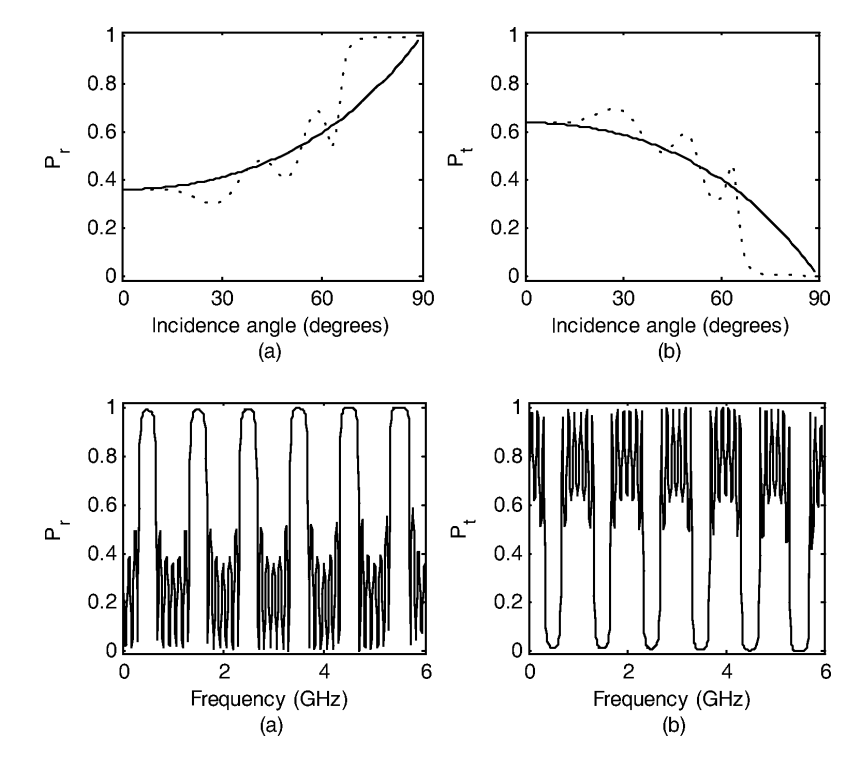


Fig. 6. Reflected and transmitted powers of the seven frequency dispersive DNG stacks versus the incidence angle at the operation frequency.

Fig. 7. Reflected and transmitted powers for the seven frequency dispersive DNG stacks against the frequency at normal incidence with  $f_{\rm epH}=19$  GHz,  $f_{\rm epL}=8$  GHz, and  $f_{\rm mpH}=f_{\rm mpL}=7$  GHz.

Figure 5 depicts the reflected and transmitted powers against the frequency at normal incidence with  $f_{\text{epH}} = 10 \text{ GHz}, f_{\text{epL}} = 4 \text{ GHz}, \text{ and } f_{\text{mpH}} = f_{\text{mpL}} =$ 3 GHz. Here,  $f_{\rm epH}$  is increased from 5 GHz to 10 GHz, to observe the effect of the plasma frequency. As it is observed from Fig. 5, the frequency response of  $P_r$  and  $P_{\rm t}$  is similar with Figure 2.  $P_{\rm r}$  acts as a band-pass filter between the frequency bands 0.3-0.7 GHz and 1.3-1.7 GHz. In turn,  $P_t$  closes to unity between the ranges of 0-0.3 GHz, 0.7-1.3 GHz, and 1.7-2 GHz, and it acts as a saw-comb filter. Comparing Fig. 2 and Fig. 5, one can see that there is a small difference between the frequency bands and it can be neglected. Thus, the frequency dispersive DNG stacks have not fixed scattering characteristics due to the variable plasma frequencies. In addition, the same scattering characteristics as in the hypothetical non-dispersive DNG stacks can be obtained by arranging the plasma frequencies of the frequency dispersive DNG stacks.

Figure 6 illustrates the reflected and transmitted powers versus the incidence angle at the operation frequency. The solid line refers to  $P_{\rm r}$  and  $P_{\rm t}$  with  $f_{\rm epH}=10$  GHz,  $f_{\rm epL}=4$  GHz, and  $f_{\rm mpH}=f_{\rm mpL}=3$  GHz and the dashed line with  $f_{\rm epL}=f_{\rm mpL}=f_{\rm mpH}=\sqrt{2}$  GHz and  $f_{\rm epH}=\sqrt{10}$  GHz. As it is seen from the solid lines,

 $P_{\rm r}$  monotonically increases and  $P_{\rm t}$  monotonically decreases with the angle of incidence. The transmitted power is dominant up to 45° and full reflection occurs at 90°. Note that the same response as in Fig. 3 is obtained when the plasma frequencies are arranged as  $f_{\rm epL} = f_{\rm mpL} = f_{\rm mpH} = \sqrt{2}$  GHz and  $f_{\rm epH} = \sqrt{10}$  GHz, as seen from the dashed lines.

# 3.3. Example III

In the last example, the effects of the plasma frequencies on the reflected and transmitted powers are presented. The seven DNG stacks are again considered with the same parameters as in the previous example except for the plasma frequencies. Here, the plasma frequencies are arranged as  $f_{\rm epH}=19$  GHz,  $f_{\rm epL}=8$  GHz, and  $f_{\rm mpH}=f_{\rm mpL}=7$  GHz.

Figure 7 shows the reflected and transmitted powers as a function of the frequency at normal incidence with  $f_{\rm epH}=19$  GHz,  $f_{\rm epL}=8$  GHz, and  $f_{\rm mpH}=f_{\rm mpL}=7$  GHz. There are multiple bandwidths in which the reflected power acts as a band-pass filter. There are also multiple frequency bands for the transmitted power, which shows a saw-comb filter characteristic. It can be said that the structure can be utilized as a multi-band-

pass and multi-saw-comb filter. Furthermore, the stop band regions in Fig. 2b can be narrowed by arranging the structure parameters and plasma frequencies. Thus, the structure can be used as a multi-notch filter.

It is confirmed that similar numerical results given in Figs. 2-7 can easily be obtained for the incident wave with parallel polarization.

### 4. Conclusions

In this paper, scattering characteristics of stratified double negative stacks which are realized using the frequency dispersive cold plasma medium are presented in detail. The DNG stacks are embedded between two DPS media, and the incident electric field is assumed to be a plane electromagnetic wave with any arbitrary polarization. The other fields inside and outside the DNG stacks are obtained using the Maxwell's equations. Also, the required equations of the DNG stack and the cold plasma medium are given in the theory. Then, the problem of electromagnetic wave propagation through the stratified DNG stacks is solved using the transfer matrix method to obtain the incident, reflected and transmitted powers. Finally, the computations of the powers for the hypothetical non-dispersive

- DNG stacks and the frequency dispersive DNG stacks, using a cold plasma medium, are demonstrated in numerical results. Also, electromagnetic filter applications of DNG materials are examined in these results. It can be said that from the numerical results, the hypothetical non-dispersive DNG stacks act as band-pass and saw-comb filters at some frequency regions for the given example. In turn, the frequency dispersive DNG stacks have no stable scattering characteristics due to the changeable plasma frequencies and frequencydependent parameters. But, the same scattering characteristics as in the hypothetical non-dispersive DNG stacks can be provided by re-arranging the plasma frequencies. Furthermore, the frequency dispersive DNG stacks can be arranged to show the multi-band-pass, multi-saw-comb, and multi-notch filter characteristics. Thus, the structure can be used as electromagnetic filters at some frequency bands. Design of these filters can be performed using the numerical results obtained here.
- The DNG stack can also be realized by using a medium different from the cold plasma. Thus, this study can be extended for periodic frequency dispersive structures distinct from the configuration considered here.
- [1] V. G. Veselago, Sov. Phys. Usp. 10, 509 (1968).
- [2] J. B. Pendry, A. J. Holden, W. J. Stewart, and I. Youngs, Phys. Rev. Lett. 76, 4773 (1996).
- [3] J.B. Pendry, A.J. Holden, D.J. Robbins, and W.J. Stewart, IEEE Trans. Microwave Theory Tech. 47, 2075 (1999).
- [4] D. R. Smith, W. J. Padilla, D. C. Vier, S. C. Nemat-Nasser, and S. Schultz, Phys. Rev. Lett. 84, 4184 (2000)
- [5] R. A. Shelby, D. R. Smith, and S. Schultz, Science 292, 77 (2001).
- [6] P. M. Valanju, R. M. Valser, and A. P. Valanju, Phys. Rev. Lett. 88, 187401-1 (2002).
- [7] J.B. Pendry and D.R. Smith, Phys. Rev. Lett. 90, 029703–1 (2003).
- [8] J. A. Kong, Prog. Electromagn. Res. 35, 1 (2002).
- [9] N. Engheta, in: Advances in Electromagnetics of Complex Media and Metamaterials, NATO Science Series, Proceedings of the NATO Advanced Research Workshop in Marrakech (Bianisotropics'2002) (Eds. S. Zouhdi, A. H. Sihvola, M. Arsalane), Kluwer Academic Publishers, Inc., Dordrecht 2002, p. 19.
- [10] W. C. Chew, Prog. Electromagn. Res. 51, 1 (2005).
- [11] C. Sabah, G. Ögücü, and S. Uckun, IV. Interna-

- tional Workshop on Electromagnetic Wave Scattering EWS'2006, Gebze Institute of Technology, Gebze, Kocaeli, Turkey 2006, p. 11.61.
- [12] C. Sabah, G. Ögücü, and S. Uckun, J. Optoelectron. Adv. Mat. 8, 1925 (2006).
- [13] Special issue on "Metamaterials", IEEE Trans. Antennas Propag. 51, 2545 (2003).
- [14] J. B. Pendry, Phys. Rev. Lett. 85, 3966 (2000).
- [15] T. J. Cui and J. A. Kong, Phys. Rev. B 70, 205106-1 (2004).
- [16] D. R. Smith and N. Kroll, Phys. Rev. Lett. 85, 2933 (2000).
- [17] D. R. Smith, D. C. Vier, N. Kroll, and S. Schultz, Appl. Phys. Lett. 77, 2246 (2000).
- [18] R. A. Shelby, D. R. Smith, S. C. Nemat-Nasser, and S. Schultz, Appl. Phys. Lett. 78, 489 (2001).
- [19] R. W. Ziolkowski and E. Heyman, Phys. Rev. E 64, 056625-1 (2001).
- [20] M. K. Karkkainen, Phys. Rev. E 68, 026602-1 (2003).
- [21] Y. Shi, Y. Li, and C.-H. Liang, Microwave Opt. Technol. Lett. 48, 57 (2006).
- [22] D. H. Staelin, A. W. Morgenthaler, and J. A. Kong, Electromagnetic Waves, Prentice Hall International Editions, New Jersey 1994.